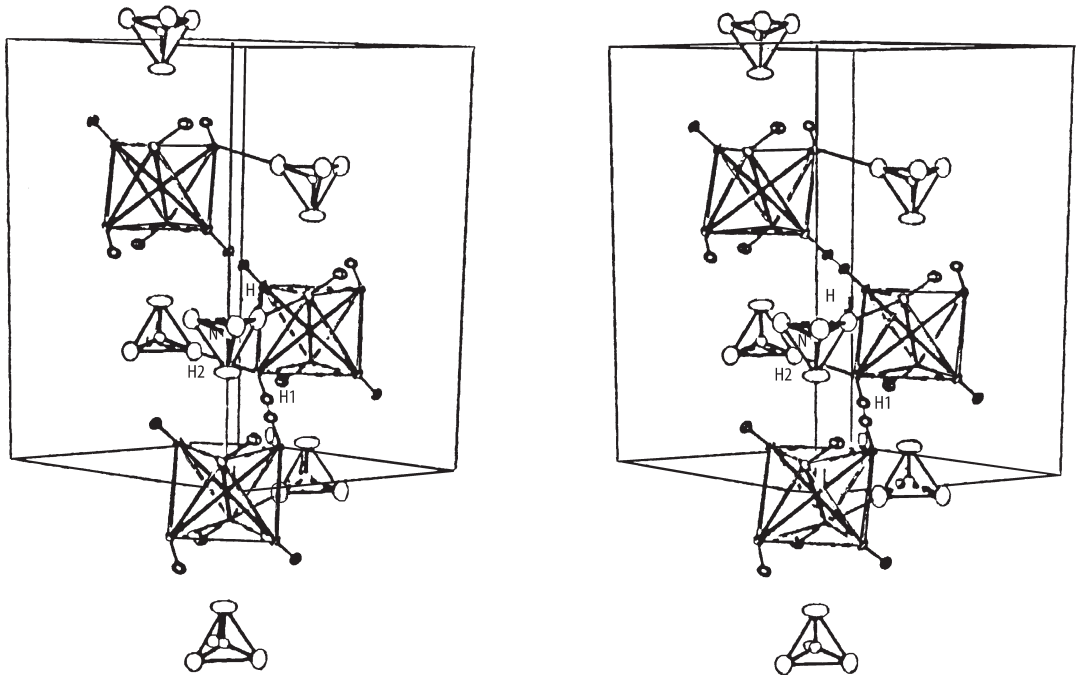

Fig. M26-ii-001. $(NH_4)_2H_3IO_6$. Stereoscopic view of the unit cell contents [80Tic].

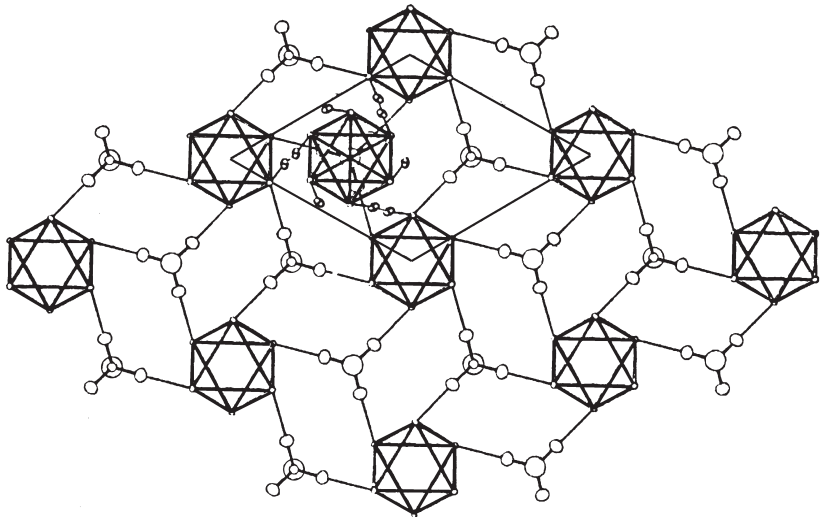

Fig. M26-ii-002. $(NH_4)_2H_3IO_6$. Hydrogen bonds network viewed along *c* [80Tic]. Hydrogen bonds between NH_4 tetrahedron and IO_6 octahedron are intralayer bonding, those between two IO_6 octahedra are interlayer bonding.

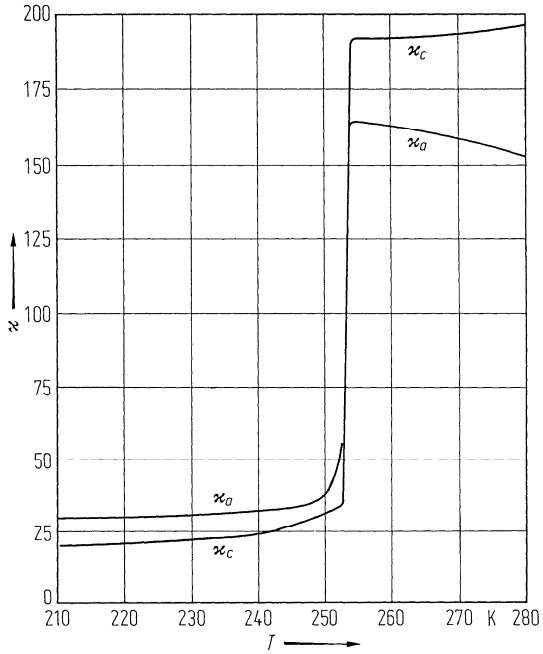

Fig. M26-ii-003. $(NH_4)_2H_3IO_6$. κ_a, κ_c vs. T [76Roo]. κ_a, κ_c: static dielectric constants.

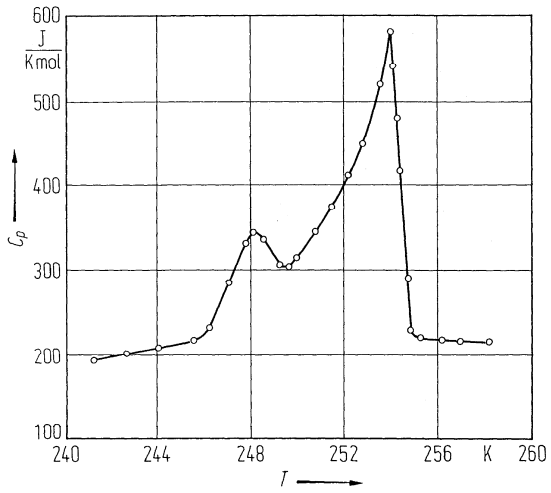

Fig. M26-ii-004. $(NH_4)_2H_3IO_6$. C_p vs. T [45Bae].

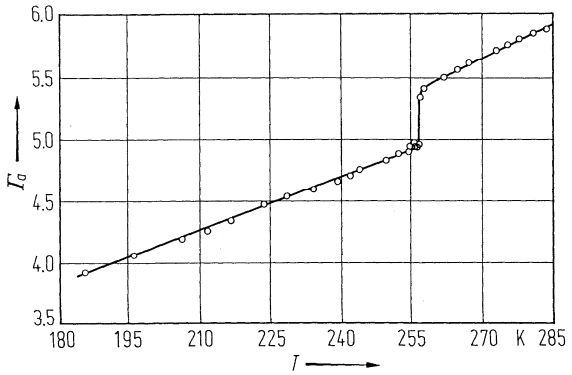

Fig. M26-ii-005. $(NH_4)_2H_3IO_6$. Γ_a vs. T [76Roo]. Γ_a: birefringence with polarization $\boldsymbol{E} \parallel \boldsymbol{c}$ which is expressed as path difference in units of wavelength used (λ = 588 nm).

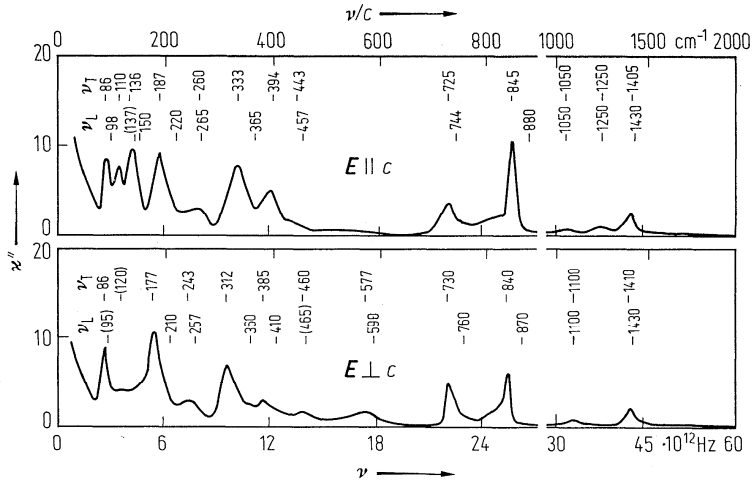

Fig. M26-ii-006. $(NH_4)_2H_3IO_6$. κ'' vs. ν [76Roo]. T = RT. κ'' was obtained from infrared reflectivity data by using Kramers-Kronig analysis. Frequencies of transverse (ν_T) and longitudinal (ν_L) modes are indicated in units of cm^{-1}.

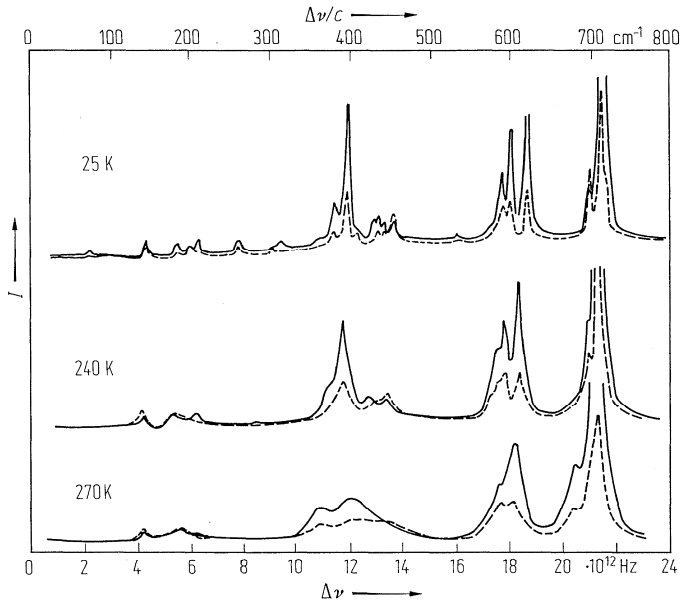

Fig. M26-ii-007. $(NH_4)_2H_3IO_6$. I vs. $\Delta\nu$ [76Pou]. I: Raman scattering intensity. Solid lines: A-modes observed in the scattering geometry $X(ZZ)Y$. Dotted lines: E-modes observed in the scattering geometry $X(YX)Y$ or $X(YZ)Y$. Parameter: T.

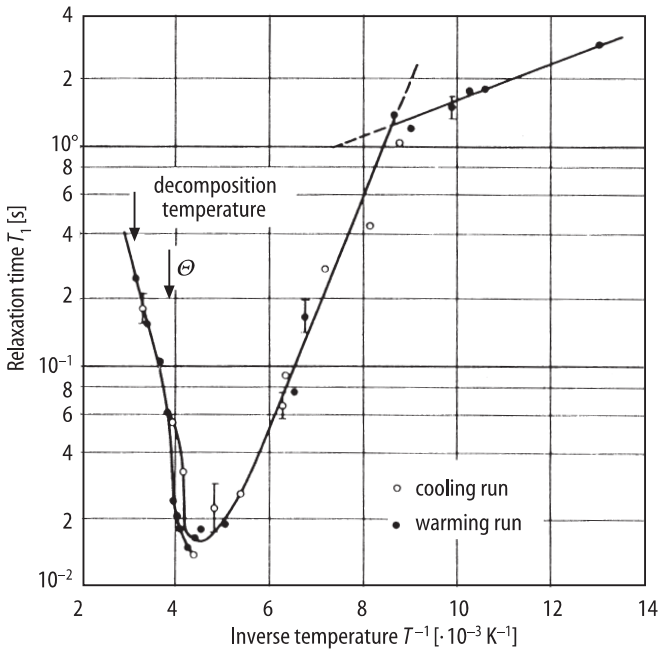

Fig. M26-ii-008. $(NH_4)_2H_3IO_6$. T_1 vs. $1/T$ [62Mil]. T_1: spin-lattice relaxation time for proton. $f = 30$ MHz.

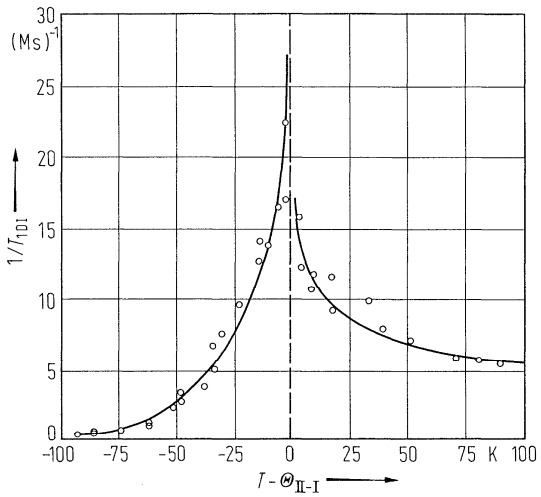

Fig. M26-ii-009. $(NH_4)_2H_3IO_6$. $1/T_{1\,DI}$ vs. $T - \Theta_{II-I}$ [73Bli]. $T_{1\,DI}$: dipolar-frame spin-lattice relaxation time for iodine.